ISTANBUL TECHNICAL UNIVERSITY ★ GRADUATE SCHOOL

OPTICAL AND MICROMECHANICAL DESIGN AND CHARACTERIZATION OF A LASER SCANNING CAPSULE ENDOSCOPE UNIT

M.Sc. THESIS

İsraa SALAHELDIN

Department of Physics Engineering

Physics Engineering Programme

JUNE 2021

ISTANBUL TECHNICAL UNIVERSITY ★ GRADUATE SCHOOL

OPTICAL AND MICROMECHANICAL DESIGN AND CHARACTERIZATION OF A LASER SCANNING CAPSULE ENDOSCOPE UNIT

M.Sc. THESIS

İsraa Salaheldin
509181111

Department of Physics Engineering

Physics Engineering Programme

Thesis Advisor: Prof. Dr. Günay Başar
Thesis Co-Advisor: Assoc. Prof. Onur Ferhanoğlu

JUNE 2021

ISTANBUL TEKNİK ÜNİVERSİTESİ ★ LİSANSÜSTÜ EĞİTİM ENSTİTÜSÜ

LAZER TARAMALI KAPSÜL ENDOSKOP ÜNİTESİNİN OPTİK VE MİKROMEKANİK TASARIM VE KARAKTERİZASYONU

YÜKSEK LİSANS TEZİ

İsraa Salaheldin
(509181111)

Fizik Mühendisliği Anabilim Dalı

Fizik Mühendisliği Programı

Tez Danışmanı: Prof. Dr. Günay Başar
Eş Danışman: Doç. Dr. Onur Ferhanoğlu

Haziran 2021

İsraa D. S. Salaheldin, a M.Sc. student of İTU Graduate School 509181111, successfully defended the thesis entitled “Wireless Laser Scanning Capsule Endoscopy”, which she prepared after fulfilling the requirements specified in the associated legislations, before the jury whose signatures are below.

Thesis Advisor :	**Prof. Dr. Günay Başar** İstanbul Technical University	.....
Co-advisor :	**Prof.Dr. Onur Ferhanoğlu** İstanbul Technical University	.....
Jury Members :	**Prof. Dr. Gönül Eryürek** Istanbul Technical University	.....
	Dr. Yiğit Dağhan Gökdel Bilgi University	.....
	Dr. Baykal Sarıoğlu Bilgi University	.....

Date of Submission : 10 JUNE 2021
Date of Defense : 29 JUNE 2021

To my spouse and cat,

FOREWORD

I would like to thank my advisor Prof. Dr. Günay Başar for his help and motivation during my work. In addition, I would like to express my gratefulness to my Co-Advisor Assoc. Prof. Onur Ferhanoğlu from Electronics and Communication Engineering Department of Istanbul Technical University for giving me the chance to work in his Electro-Optical Devices Laboratory (EDL), where I conducted my thesis project under his guidance. I would like to thank him for the endless support and patience he showed me during the past three years I spent in EDL where I enhanced my experimental skills and teamwork capabilities, and I am very grateful that I had the chance to know and work with such a productive instructor.
Finally, I would thank my closest, lifelong friend and husband Mustafa Salih ZÖĞ for always giving me encouragement and strength to handle every difficulty in my life, and always being the first factor in my success. Wish him a good luck in his thesis presentation and in future career.

During the course of this thesis, I was supported by scholarship from TUBITAK grant no:119E224 project.

JUNE 2021 İsraa Salaheldin

TABLE OF CONTENTS

Page

ABBREVIATIONS

GI **:** Gastrointestinal
MMF **:** Multi-Mode Fiber
SMF **:** Single-Mode Fiber
OBJ **:** Objective Lens
M **:** Mirror
SLA **:** Stereolithography
SLS **:** Selective Laser Sintering
FDM **:** Fused-Deposition Modelling
ABS **:** Hierarchical Cluster Analysis
PLA **:** Polylactic Acid
OCT **:** Optical Coherence Tomography

SYMBOLS

w	**:** Width
$\mathbf{D_{Lens}}$	**:** Diameter of the lens
$\mathbf{D_{Actuator}}$	**:** Diameter of the actuator
$\boldsymbol{\theta}$	**:** Angle theta
$\boldsymbol{\lambda}$	**:** Wavelength
t	**:** Time
T	**:** Period
$\boldsymbol{\delta}$	**:** Optical Resolution
NA	**:** Numerical Aperture
R	**:** Radius
L	**:** Length

LIST OF TABLES

Page

LIST OF FIGURES

Page

Optical and Micromechanical Design and Characterization of a Laser Scanning Capsule Endoscope Unit

SUMMARY

In this study we proposed the utilization of laser scanning in wireless capsule endoscopy to provide high-resolution imaging at multiple depth sections throughout the gastrointestinal tract. The proposed device, provides a confocal imaging, consist of a laser and a photo detector, a 3D printed focus adjusting actuator, a micro-motor for circumferential scanning, and batteries for energy source. It also involves a conformal antenna to transmit the acquired data to an external receiver unit and an integrated circuit to administer the entire operation. In this thesis, -held in Electro-Optical Devices Laboratory- of ITU, we illustrate the design, manufacturing, and characterization of the focus adjusting actuator. The actuator has a spiral flexure, carrying a lens and two magnets at its center to undergo focusing through electromagnetic actuation. The interplay between the spiral flexure length and the lens size is investigated for optimal performance. An external coil is utilized to drive the lens actuator with a low power (~ 5mW) to acquire data from targets placed at multiple depths. Discussion on the integrated circuit and antenna design is also provided. With further development, the proposed device can be adapted for the clinical environment. At the end of the study, we could get data from different targets placed at different distances from the lens, representing tissues at different depths. The frequency response of the focus adjusting actuator was scanned and the first mode of the actuator was found experimentally and by simulations. The coil was driven with an exterinal function generator, and at the resonance frequency ~23Hz, 100 μm displacement was achieved by only 1 mW power, which is considerably low. Moreover, the spot size at the focus was analyzed and calculated. This project is supported by TUBITAK (The Scientific and Technological Research Council of Turkey) grant No:119E224, and the study was submitted to Sensors and Actuators A Journal, in May 2021.

Lazer Taramalı Kapsül Endoskop Ünitesinin Optik ve Mikromekanik Tasarımı ve Karakterizasyonu

ÖZET

Endoskopik prosedürler, sağlıksız doku oluşumlarını (polipler, ülserler, tümörler vb.) Teşhis etmeyi amaçlamaktadır. Endoskopi yapılacak hasta işlemden bir veya birkaç gün önce başlayarak diyete girer. Ayrıca, prosedür hasta için oldukça rahatsız edici olduğundan rahatsızlığı azaltmak için bir sakinleştirici verilir. Konvansiyonel endoskopi, kanser öncesi dokuların erken teşhisinde hayat kurtarıcı olsa da, tabii ki hasta için oldukça rahatsız edici bir işlemdir. Ayrıca özofagustan endoskopik bir işlem sadece duodenuma, anal kaviteden yapılan bir işlem ise ince bağırsağa kadar ulaşabilir. Bu nedenle tüm gastrointestinal (GI) sistemin tek endoskopik prosedürle görüntülenmesi mümkün değildir. Konvansiyonel endoskopinin hastaya getirdiği rahatsızlık, tüm GI yoluna ulaşmadaki sınırlamaları ile birlikte, kapsül veya hap endoskoplarının hızlı gelişimini kolaylaştırdı. Dahası, prosedür bir hap yutmak kadar rahattır, bu nedenle sakinleştirici gerekmez. Hasta konforundaki avantajları ve görüntülenebilen kanal uzunluğu ile kapsül endoskopların yakın gelecekte yaygınlaşması beklenmektedir. Çoğu kapsül endoskop, CMOS / CCD kameralar içerir ve katedilen yol boyunca görüntüler çeker. Görüntüler bir anten aracılığıyla dışarıya yayılır. Bununla birlikte, kameralarla yakalanan görüntüler yalnızca yüzeyle ilgili sınırlı bilgi sağlar ve hücresel düzeyde patolojik bilgilerin çıkarılamayacağı düşük çözünürlüğe sahiptir. Çözünürlüğü ve dokunun çoklu derinliklerini görüntülemeyi iyileştirme çabasıyla, MIT ve Mass General Hospital Araştırmacıları tarafından, dokunun çoklu derinliklerinde optik çözünürlüğü ve görüntü kalitesini iyileştirmek için görüntüleme yöntemi olarak optik koherens tomografiyi (OCT) kullanan bağlı kapsül endoskopları geliştirilmiştir. Yine de, GI yolunun dışındaki herhangi bir elektriksel veya optik bağlantı, erişilebilirlik açısından geleneksel endoskopinin dezavantajlarını miras alır.

Bu çalışma, gastrointestinal sistem boyunca sınırsız erişim ile yüksek çözünürlüklü ve çok katmanlı görüntülemeye yönelik kablosuz bir kapsül endoskopu önermektedir. Önerilen cihaz, lazer taramalı konfokal görüntüleme kullanır. Işık göndermek ve almak için optik bileşenlerden (lazer, fotodiyot, yansıtıcı prizma, odaklama lensi) ve doku üzerindeki ışını taramak için aktüatörlerden (3D baskılı lens aktüatör ve mikro motor) oluşur. Dahası, kapsülü çalıştırmak ve sistemin farklı bölümlerinde operasyonu yürütmek için elektronik bileşenlerden (piller, entegre devre blokları) yararlanılır. Son olarak, elde edilen verileri alıcı birimine iletmek için uygun bir anten, kapsülün dışına yerleştirilir. Fotodiyotun mikrometrik (~ 100 μm x 100 μm) boyutu odak dışı ışığı reddetmek için bir iğne deliği görevi gördüğünden, konfokal görüntüleme işlemi sağlanır.

3D baskı teknolojisi, hızlı üretim kapasitesi (özellikle geliştirme aşamasında), orta özellik boyutu ve düşük maliyeti sayesinde aktüatör geliştirmeye çekici bir alternatif haline geldi. 3D yazıcılar, robotikte, optik fiberlerin ve aktüatörlerin imalatında parça ve bileşenlerin basılmasında yer aldı. Yüksek maliyetli ve hacimli makinelere bağlı kalmadan, 3D yazıcılar opto-tıbbi görüntüleme sistemlerinde kullanılmak üzere dinamik yapılar oluşturmak için çekici bir araç haline geliyor. Özellikle

mikrosistemlerde ve mikroakışkanlarda, 3D yazıcılar büyük bir rol oynar. Daha önce de belirtildiği gibi, düşük maliyet ve hızlı üretim nedeniyle parçalar veya bazen tüm modeller 3D olarak yazdırılır. Seçici Lazer Sinterleme (SLS) ve Streolitografi (SLA) gibi farklı 3B baskı teknolojisi türleri vardır, sıvı reçineden sert nesneler oluşturmak için lazer ışını gibi radyasyon kaynaklarını kullanır. Bu yöntemler, yüksek çözünürlük ve temiz yüzey kalitesi gibi avantajlarla öne çıkıyor. Oysa, Fused-Deposition Modeling (FDM), daha az karmaşık baskı yöntemi ve daha ucuz cihaz parçaları nedeniyle piyasada en çok bulunan 3D baskı makinesidir. Bu cihaz ısıtma prensibine göre çalışır. Bir polimer filament, ABS (akrilonitril bütadien stiren) veya PLA (polilaktik asit), (200-220 ℃) derecelik nozüle sıvı halde verilir ve XY düzleminde hareket eden tablaya döküldükten sonra katılaşır. Cihazın hafıza katına yüklenen geometri şekli üzerinde basım gerçekleşir.

Bu tezde, lazer taramalı kablosuz kapsül endoskop, gastrointestinal sistem boyunca farklı derinliklerden yüksek çözünürlüklü görüntüleme sağlamak için kullanılmasını önerdik. Önerilen cihaz, bir lazer ve bir fotodetektörü, bir 3D baskılı odak ayarlama aktüatörü, çevresel tarama için bir mikro motor ve enerji kaynağı için pillerden oluşan bir konfokal görüntüleme sağlar. Ayrıca, elde edilen verileri harici bir alıcı birimine iletmek için uyumlu bir anten ve tüm operasyonu yönetmek için bir entegre devre içerir. İTÜ Elektro-Optik Cihazlar Laboratuvarı'nda gerçekleştirilen bu tezde, odak ayarlama aktüatörünün tasarımını, üretimini ve karakterizasyonunu gösteriyoruz. Aktüatör, elektromanyetik eyleme yoluyla odaklanmak için merkezinde bir mercek ve iki mıknatıs taşıyan spiral bir şekile sahiptir. Optimum performans için spiral uzunluğu ile lens boyutu arasındaki etkileşim araştırılır. Birden fazla derinliğe -farklı mesafelere- yerleştirilmiş hedeflerden veri elde etmek için lens aktüatörünü düşük bir güçle (~ 5mW) çalıştırmak için harici bir bobin kullanılır. Entegre devre ve anten tasarımı ile ilgili tartışma da sağlanmaktadır. Daha fazla geliştirme ile, önerilen cihaz klinik ortama uyarlanabilir. Çalışmanın sonunda, merceğe farklı mesafelerde yerleştirilmiş, farklı derinliklerdeki dokuları temsil eden farklı hedeflerden veri alabildik. Odak ayarlama aktüatörünün frekans tepkisi tarandı ve aktüatörün ilk modu deneysel olarak ve simülasyonlarla bulundu. Bobin, harici bir fonksiyon üreteci ile çalıştırıldı. Rrezonans frekansında (~23Hz'de) çalıştırarark, 100 μm yer değiştirme elde edildi. Bu yer değiştirme miktarı oldukça düşük olan yalnızca 1 mW güçle sağlandı. Ayrıca odak boyutu analiz edildi ve hesaplandı. Bu proje, TÜBİTAK (Türkiye Bilimsel ve Teknolojik Araştırma Kurumu) hibe No: 119E224 tarafından desteklenmekte olup, çalışma Mayıs 2021'de Sensors and Actuators A dergisi'ne sunulmuştur.

Bu tezde üç farklı deney seti yaptık. ilki, 3D baskılı aktüatörün mekanik davranışının test edilmesiyle ilgiliydi. Önerilen 3 aktüatör tasarımının (360, 540 ve 720 derece) rezonans frekansını belirlemeyi hedefledik ve bunu harici bobini bir fonksiyon jeneratörüyle sürerek ve aktüatörün yer değiştirmesini ölçmek için uygulanan voltaj miktarını değiştirerek yaptık.

İkinci deney grubu, deneylerde kullanılan lazer ışığının odak noktasının karakterizasyonunu içeriyordu. Amaç, spot boyutunu hesaplamak ve ayrıca eyleme sırasındaki spot değişikliklerini görmekti. Ayrıca bu deneyler sırasında istenen yer değiştirme için gereken güç miktarı da belirlenmiştir.

Son olarak ve en önemli deney seti, farklı derinliklerde yerleştirilmiş hedeflerden veri almak hakkındaydı. Mercekten farklı konum ve mesafelere yerleştirilmiş farklı hedeflerden aynı anda veri elde etmeyi amaçladık. i) hedefler lensten eşit uzaklıkta, ii) hedefler eşit uzaklıkta ancak aktüatör AÇIK, iii) hedefler farklı mesafelerdeydi ve aktüatör AÇIK durumdaydı gibi deneyler yaptık. Bu veriler ve sonuçlar bu tez boyunca gösterilecek ve sunulacaktır.

1. INTRODUCTION

Conventional endoscopic procedures, aim to diagnose unhealthy tissue formations (polyps, ulcers, tumors, etc.). Patient to undergo endoscopy goes through a diet starting one or more days before the procedure. Furthermore, the procedure is quiet uncomfortable for the patient, so a sedative is given to mitigate the discomfort. Though conventional endoscopy is a life saver in early detection of pre-cancerous tissues, obviously it is also comfortless for the patient. Moreover an endoscopic procedure through the esophagus can only reach till duodenum, while a procedure through the anal cavity can access till the small bowel [1]. Thus imaging the entire gastrointestinal (GI) tract with single endoscopic procedure is not feasible. The discomfort that conventional endoscopy brings to the patient, along with its limitations in reaching the entire GI tract facilitated the rapid development of capsule or pill endoscopes. Moreover, the procedure is as comfortable as swallowing a pill, thus no sedatives are required. With its advantages in patient comfort and the length of tract that can be imaged, capsule endoscopes are expected to become wide spread in near future [2]. Most capsule endoscopes embark CMOS / CCD cameras and shoot images along the path traveled. The images are propagated outside via an antenna. However, images that are captured with cameras provide limited information only regarding the surface, and possess low resolution from which cellular level pathological information cannot be deduced [3,4]. In an effort to improve resolution and image multiple tissue depths, tethered capsule endoscopes have been developed by MIT and Mass General Hospital Researchers utilizing optical coherence tomography (OCT) as the imaging modality to improve optical resolution and image quality at multiple tissue depths [5]. Yet, any electrical or optical connection out of the GI tract inherits disadvantages of conventional endoscopy in terms of accessibility.

1.1 3-D Printing Technology

3D printing technology has become an appealing alternative to develop actuators, owing to its rapid manufacturing capability (particularly at development stage), moderate feature size, and low cost. 3D printers took place in printing parts and components in soft robotics, [6], in fabrication of optical fibers [7], and actuators [8]. Without relying on high cost and bulky machinery, 3D printers are becoming an appealing tool to build dynamic structures for use in opto-medical imaging systems. In microsystems and microfluidics especially, 3D printers play a huge role [9]. As mentioned before, due to the low cost and the fast manufacturing, parts or sometimes the whole models are 3D printed [10]. There are different types of 3D printing technology such as the Selective Laser Sintering (SLS), and Streolithography (SLA), use radiation sources such as laser beam to create rigid objects from liquid resin [11]. These methods stand out for advantages like high resolution, and clean surface finish [12]. Whereas, Fused-Deposition Modelling (FDM) is the most commercially available 3D printing machine, due to its less complex printing method and cheaper device parts [13]. This device works by heating principle. A polymer filament, ABS (acrylonitrile butadiene styrene) or PLA (polylactic acid) is delivered to the nozzle ($200 - 220$ ℃) in a liquid form and solidifies onces it is poured on the table which in turns, moves in the XY plane depending on the geometry shape inserted to the memory of the device [14]. Figure 1.1 below shows the 3D printing device (Ender Pro 3) presented in our laboratory that made it possible to print the parts of the capsule illustrated in this thesis.

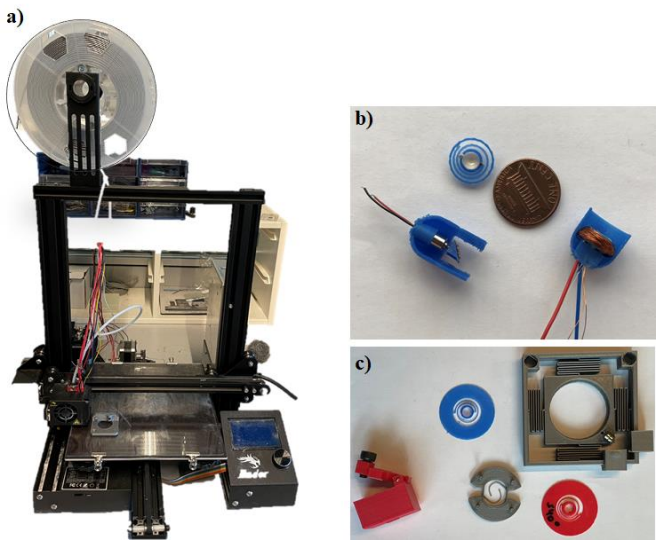

Figure 1.1 : a) the FDM machine presented in our EDL LAB. b)&c) some mechanical parts printed by the device in a) with different sizes for different functions.

1.2 Purpose of Thesis

This study proposes a wireless capsule endoscope towards high resolution and multi-layered imaging with unlimited access throughout the gastrointestinal tract. The proposed device, illustrated in Figure 1.2 employs laser-scanned confocal imaging. It consists of optical components (laser, photodiode, reflective prism, focusing lens) to send and receive light, as well as actuators (3D-printed lens actuator and micro-motor) to scan the beam on the tissue. Moreover, electronics components (batteries, integrated circuit blocks) are leveraged to power up the capsule and conduct the operation across different parts of the system. Lastly, a conformal antenna to transmit the acquired data to the receiver unit is placed outside the capsule. The confocal imaging operation is ensured, as the micrometric (~ 100 µm x 100 µm) size of the photodiode acts as a pinhole to reject the out-of-focus light.

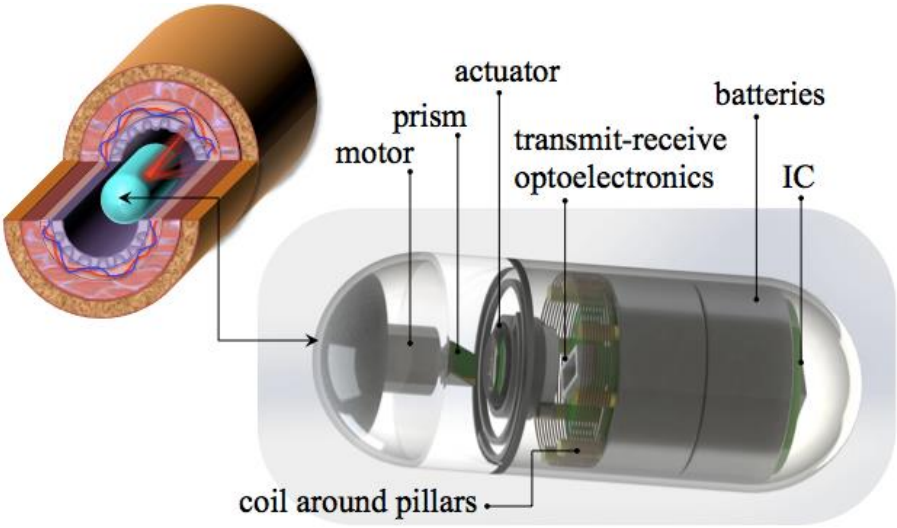

Figure 1.2 : The wireless laser scanning capsule endoscope; sketch during operation within the small intestine and internal architecture. The device comprises a rotating prism, a focus adjustment actuator, batteries, and two electronic boards (one embarking the laser and the photodiode and the other containing a transimpedance amplifier, oscillator, filter, power amplifier, and other related circuit blocks)

2. DESIGN AND FABRICATION OF THE ACTUATO

2.1 Design

The circular cross-section of the capsule led us to design the lens actuator in the form of a spiral flexure fixed to the capsule wall. The distal end of the spiral flexure is connected to a rim, in which the focusing lens is placed. The rim is also dedicated to attaching magnets to enable electromagnetic actuation via an external coil. The flexure has a square cross-section with 0.4 mm edge length, according to the capabilities of the in-house fused-deposition-modeling (FDM) device having a polylactic acid (PLA) filament. Figure 2.1.1 illustrates the geometry of three different variations of the actuator; a one-side flexure, two-side flexure, and multi-layered flexure. The overall actuator dimension spans a D_{act} = 11.4 mm diameter to fit within a 12.5 mm diameter capsule.

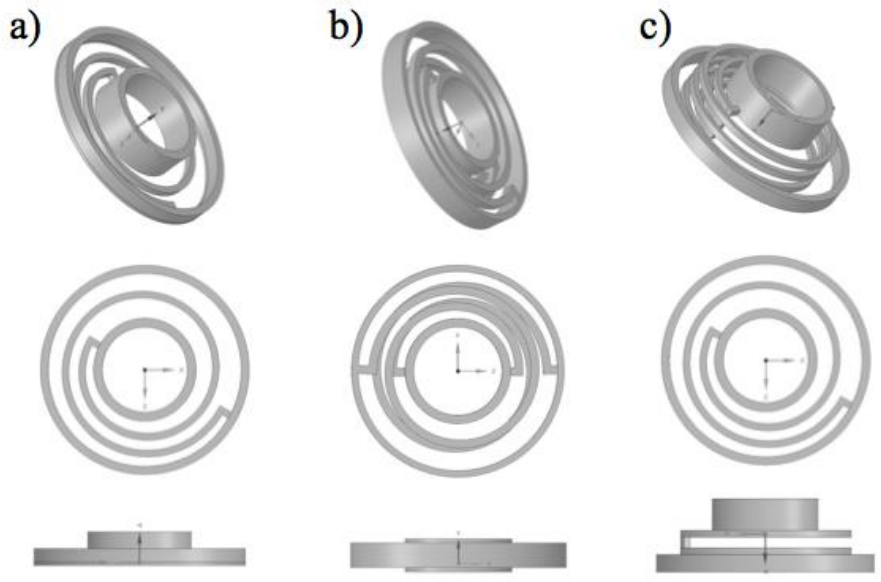

Figure 2.1.1 : Focus adjusting lens actuator designs a) one-side fixed b) two-sides fixed c) multi-layered.

We investigated the role of the flexure length on both the spring constant and the optical resolution. A longer flexure results in a compliant structure that requires less power for actuation. Conversely, using a long flexure leaves a smaller area for the lens,

thereby degrading the optical resolution. Overall, the interplay between the power budget of the capsule and the desired optical resolution enforces a selection on the flexure length. We note that the finite-element simulated (using the COMSOL software) stiffness values for various flexure length shows a similar trend with the analytical stiffness (*k*) formulation for a spiral beam [15];

$$k \propto \frac{EWH^3}{L} \tag{1}$$

where *E* is Young's Modulus of the flexure material, and *L* is the total length of the flexure. W is the width and H is the height of the flexure cross section

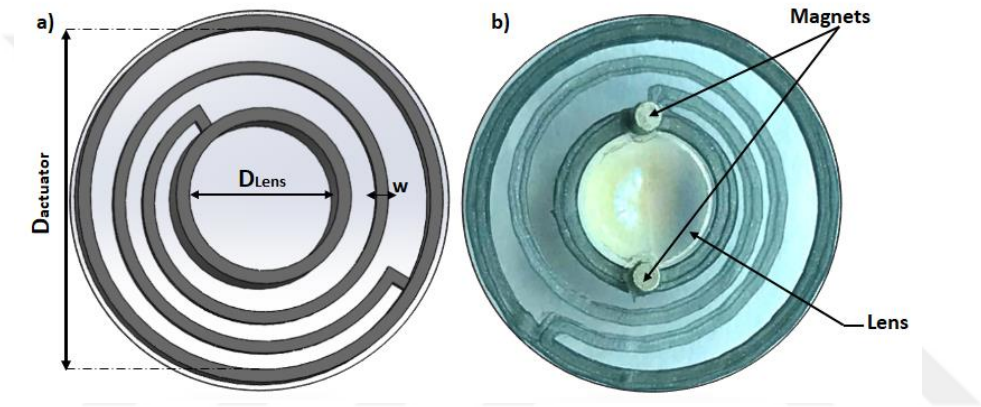

Figure 2.1.2 : The presented spiral actuator. a) CAD drawing. b) 3D printed with two magnets glued and a focusing lens (Thorlabs 354171, NA: 0.3) inserted in the middle.

Table 2.1: Dimensions of the presented actuator.

Part	Notation	Dimension
Lens	D_{Lens}	4.7 mm
Actuator Diameter	$D_{actuator}$	11.4 mm
Width of the flexure	W	0.4 mm
Angle of the Spiral	θ	540 °

The full-width half-maximum (FWHM) lateral (δ_{xy}) and axial (δ_z) optical resolution are calculated using [16] :

$$\delta_{xy} \simeq \frac{\lambda}{2NA} \tag{2}$$

$$\delta_z \simeq \frac{\lambda}{NA^2} \tag{3}$$

where λ is the wavelength of the light source and NA is the numerical aperture of the lens. Note that the NA of the lens is determined by its radius (R_{lens}) and the focused distance, d_{tissue} = 17 mm. The focused distance is the distance between the actuator lens and the small intestine surface, calculated based on the sum of the average small intestine radius of 12.5 mm [17] and the lens-to-reflective prism distance of 5 mm. Overall, the lens NA for the Archimedean spiral actuator can be written as a function of the total flexure angle (θ_f) as:

$$NA = \frac{R_{lens}}{d_{tissue}} \approx \frac{R_{act} - 4W - 2.5W.\theta_f/360\circ)}{d_{tissue}} \tag{4}$$

where W = 0.4 mm is the width of the flexure. Figure 2.1.3 illustrates the stiffness vs. optical resolution for a one-side fixed actuator design having different total flexure angles based on formulations presented in (2) and (4). A similar analysis could be carried out for a two-sides-fixed actuator and a multi-layered design without loss of generality. It is worth noting that despite offering a near-perfect out-of-plane motion (without tilts), the spring constant is significantly higher for the two-sides-fixed actuator, which would require much higher power for actuation.

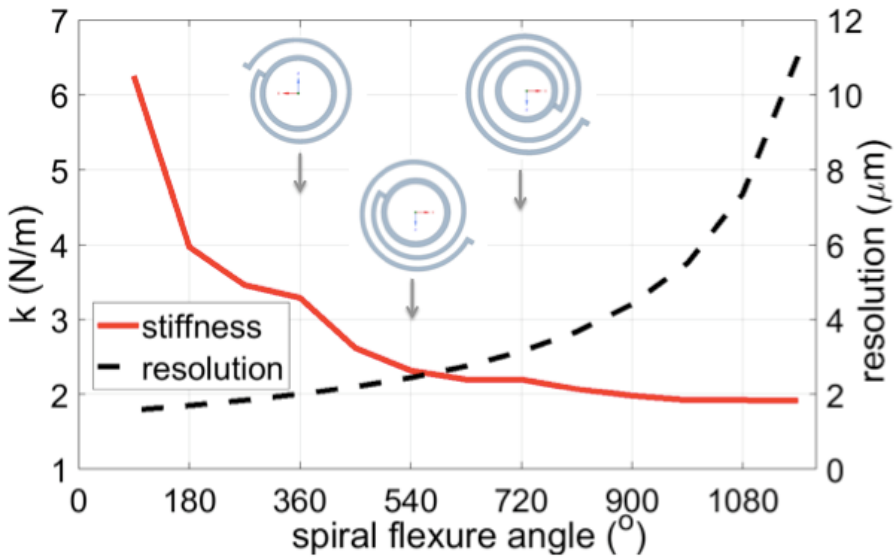

Figure 2.1.3 : Stiffness and lateral optical resolution as a function of spiral flexure angle for a one-side fixed actuator design.

Also, multi-layered actuator designs require a higher volume of support structure that may be challenging to eliminate, particularly for FDM. Yet, for other 3D printing technologies (i.e., Polyjet technology), support structures are deposited using a different material that can be etched out. Overall, based on space constraints and in-house manufacturing capabilities, we continued our testing efforts with a single-layered and 1.5 turns (540 °) spiral flexure. This leads to a theoretical lateral resolution of 2.9 μm (based on Figure 2.1.3) and an axial resolution of 50 μm (based on Eq. 3) for a source of λ = 630 nm. Calculated optical resolution values, while being larger than those of a typical bench-top laser-scanning microscope, still offer sub-cellular imaging capability at various small intestinal layers (mucosa, submucosa, and various muscle layers).

2.2 Fabrication

In this study, we have used FDM in printing the designed actuators. In all three dimensions, we were able to fabricate the features of 300 μm. Nevertheless, a significant increase in the yield of manufactured devices was observed when the feature size was increased to 400 μm.

Other parts of the capsule were also implemented to characterize the mechanical and optical components in the proposed system, as illustrated in Figure 2.2. The capsule was printed in a modular fashion. One module was the actuator itself. The second module was printed to locate the laser, and the third module was allocated for the scanner motor. The overall capsule device spanned a length of 30 mm and a radius of 12.5 mm, complying with the off-the-shelf pill endoscopes. Two neodymium magnets (1 mm height, 1 mm diameter) were attached on the rim, while an aspherical lens (Thorlabs 354171, NA: 0.3) was press-fit into the center portion of the actuator. A 200-turn copper coil, with 0.2 mm wire diameter, was wrapped around the laser casing to enable electromagnetic actuation of the actuator. A 3D-printed prism (with 4 mm edge length) was inserted into the motor shaft, on which a gold-coated silicon piece was attached for light reflection.

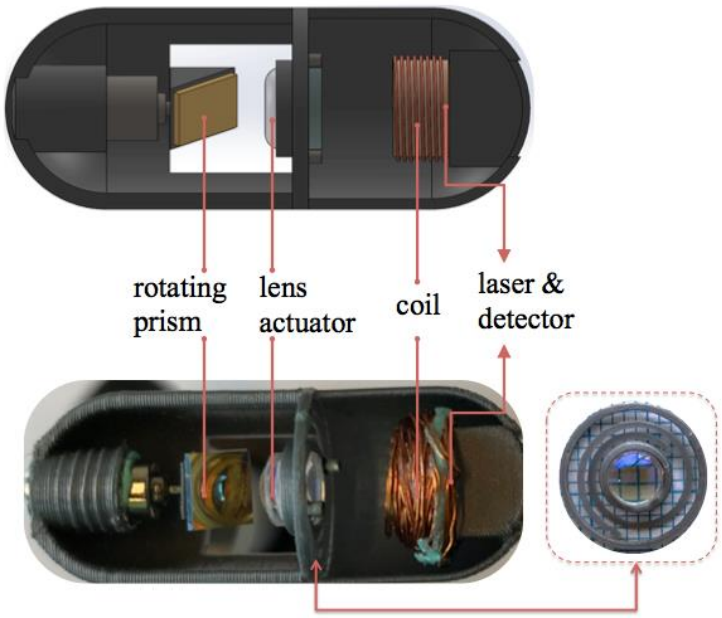

Figure 2.2 : Capsule tested in this study. Inset shows the 3D printed and lens-magnet- integrated spiral focus adjustment actuator. Besides the actuator, the capsule embarks a prism-attached motor, a laser diode, a coil wrapped around the laser diode case, and an acquisition fiber (inside the laser casing) to detect light reflecting off the target.

This study focuses on the mechanical and optical aspects of the proposed capsule endoscope architecture. Thus, neither microelectronic chips nor the antenna was involved at this stage. Consequently, the capsule is still wired where the coil is driven by an external function generator that also operates the laser and the motor. Finally, the reflected light from the target is captured via a multi-mode fiber connected to an external photodetector unit). Yet, the proposed architecture involves the microelectronics components (circuit blocks to drive the laser, actuator, motor, and sense & amplify the acquired light), whose presence will allow the device to be wire-free in future studies.

Original equipment manufacturer (OEM) laser diode and the motor were integrated within the capsule, costing only < $3. Moreover, the usage of FDM, the most inexpensive 3D printing methodology, paves the way for manufacturing each capsule at a significantly reduced cost (specifically for mass production, where integrated circuit cost is also lowered to a great extent).

3. SCAN PATTERN

The motor radially scans the laser on the tissue surface while the lens actuator alters the radius of the scan to address multiple tissue layers. The transverse optical magnification (M_T) is defined as the ratio of the image distance (d_i: distance between the focus and the lens) to the object distance (d_o: distance between the lens and the laser). Conversely, the longitudinal magnification (M_L) of an optical system is linked to the square of the transverse magnification as [18]:

$$|M_L| = M_T^2 = \left(\frac{d_o}{d_i}\right)^2 \tag{5}$$

The longitudinal magnification of our capsule system is $M_L \cong 16$. As the **extinction length** (including scattering and absorption effects) of the small intestine tissue for red and NIR wavelengths is about 1 mm [19], one needs to displace the lens by ~ ± 100 μm to address three extinction lengths , based on Eq. 5. The actuator can be excited at its resonance frequency (f_a) to decrease its power consumption. The combination of the motor scanning and resonant lens actuation leads to the following mathematical formulation for the scan pattern:

$$x(t) = d_t \sin(2\pi f_a t)\, R_t \sin(2\pi f_m t), \tag{6}$$

$$y(t) = d_t \sin(2\pi f_a t)\, R_t \cos(2\pi f_m t), \tag{7}$$

$$z(t) = v_c \mathrm{t}. \tag{8}$$

Here, *x(t)*, *y(t)*, and *z(t)* are the location of the laser spot as a function of time in three dimensions. The motor rotates at the frequency of f_m, creating a circular scan around the tissue with a radius of R_t, modeled by a sinusoidal function in the lateral (x, y) plane with a 90° phase difference. The radius of the circular scan is also a time-varying function with d_t amplitude due to the lens actuator operating at its resonance.

Moreover, the peristaltic motion causes the capsule to move at an average speed of v_c. Figure 3.1 illustrates the scan pattern in three dimensions, for R_t = 25 mm, d_t = 1.5 mm (to address a total of 3 extinction lengths), f_a = 25 Hz (based on simulated values), f_m = 125 Hz (based on experimented motor speed), and v_c = 0.23 mm/sec [20].

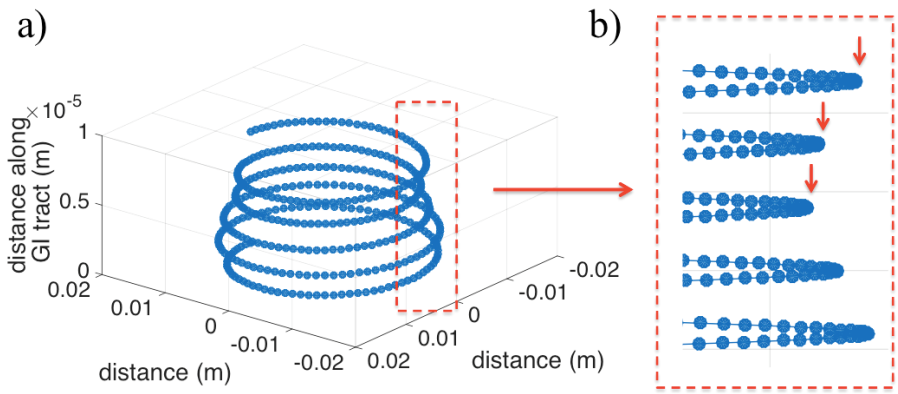

Figure 3.1 : Scan pattern in 3D; a) oblique view b) close-up view of the rectangular region in a) showcasing different tissue planes at multiple depths being addressed.

4. EXPERIMENTAL SETUP AND EXPERIMENTS

4.1 Mechanical Behavior of the Actuator

4.1.1 AC experiment

A function generator was used to drive the coil as shown in figure 4.1.1. In this way much more actuation is achieved with very low power consumption.

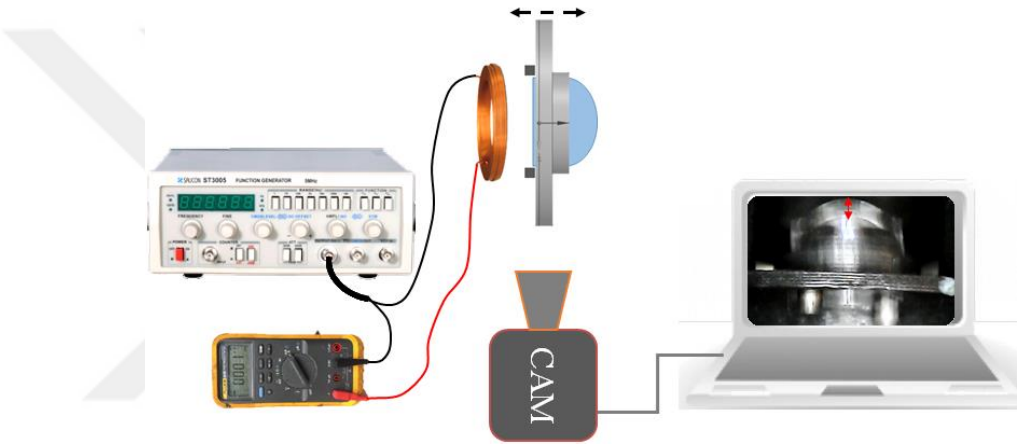

Figure 4.1.1 : The experiment setup for the frequency response of the actuators.

In this experiment, the three types of actuators illustated in figure 2.1.1 are used one after another. Their first mode resonance frequency is found, and their frequency response is plotted as a function of the displacement.

4.1.2 Modal analysis

The fundamental mode shapes of 1, 1.5, and 2-turn spiral actuators were found using COMSOL software, revealing a frequency within 27 ± 2 Hz range. While the number of turns significantly affects the spring constant, the mass of the lens embedded in each design mitigates the change in resonance frequency. Hence, an actuator with more turns is compliant and spares a smaller volume for the lens. On the contrary, an actuator with a short spiral flexure will be stiff yet reserving a larger space for the lens. As the device frequency depends on the stiffness to mass ratio, all actuators possess a similar

fundamental frequency. Figure 4.1.2 shows the first mode frequency of all three types of actuator.

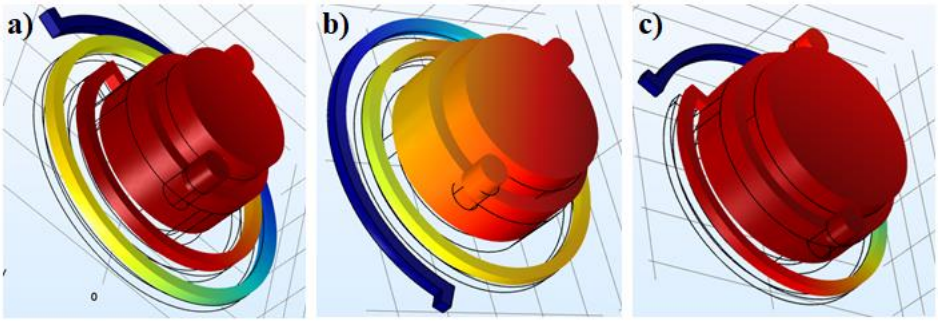

Figure 4.1.2 : Modal analysis of a)2, b)1.5, and c)1-turn one-end-fixed spiral actuators. The actuators show29 Hz, 27 Hz, 25 Hz fundamental mode frequency, respectively.

4.2 Focal Spot Characterization

The second setup shown in figure 4.2 was built to observe and characterize the focal spot of the laser light used in the capsule.

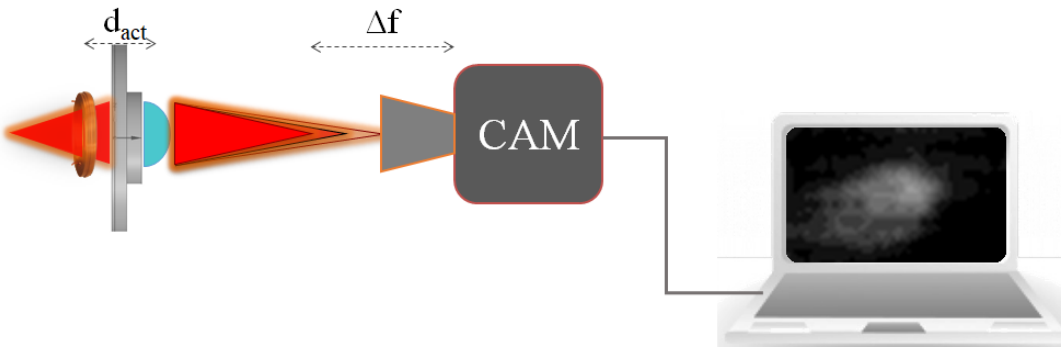

Figure 4.2 : Experiment setup for focal spot characterization

In this set of experiment, we aimed at monitoring the focal spot in terms of changing in size while actuation is on. The actuator was actuating at resonance frequency and the camera was placed 25mm away from the lens at first, then it was readjusted $\pm 2{,}5mm$ to address the focus in each of the three points as shown in figure 5.3.

4.3 Multi-depth Experiment

Figure 4.3 illustrates the experimental setup, a laser coupled into a single-mode fiber entering the capsule for laser delivery and detection (using the Thorlabs PDA36 photodetector) from the target, two mirrors at different positions (one above and the other below the capsule, whose distances were varied throughout the experiments) with respect to the capsule. The mirrors represented the target tissue.

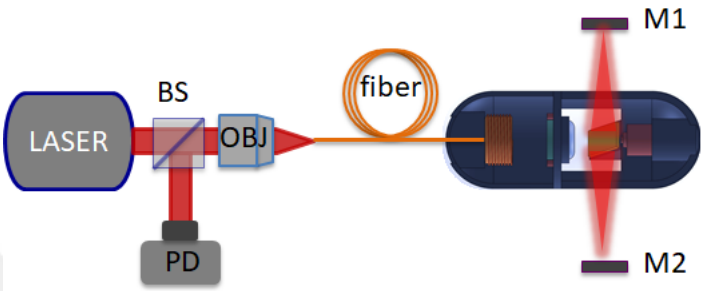

Figure 4.3 : Experimental setup, comprising a single-mode fiber for laser delivery and detection (photodetector: PD unit). A beam-splitter (BS) to separate delivered light and collected light. An objective lens (OBJ) is utilized for fiber coupling, and two mirrors (M1 and M2) were placed at two target locations.

5. RESULTS

We have measured the frequency response for 1, 1.5, and 2-turn spiral actuators using the presented setup in figure 4.1.1. A comparison of simulated –figure 4.1.2- and experimented resonance frequencies is shown in figure 5.1 and Table 5.1 We observe an error of < 13.3 % for all three devices between simulated and experimented mode frequencies and mainly attribute it to the slight difference of lens dimensions utilized in the experiments and simulations.

Table 5.1 : Comparison of simulated and experimented fundamental mode frequencies for 1, 1.5, and 2 turn spiral actuators. The error between simulated and experimented values is also depicted in the rightmost column.

	First mode frequency (Simulation)	First mode frequency (Experiment)	Error
1-turn (360°) spiral actuator	25.1 Hz	27.6 Hz	10 %
1.5-turn (540°) spiral actuator	26.8 Hz	23.7 Hz	11.5 %
2-turn (720°) spiral actuator	29.2 Hz	33.7 Hz	13.3 %

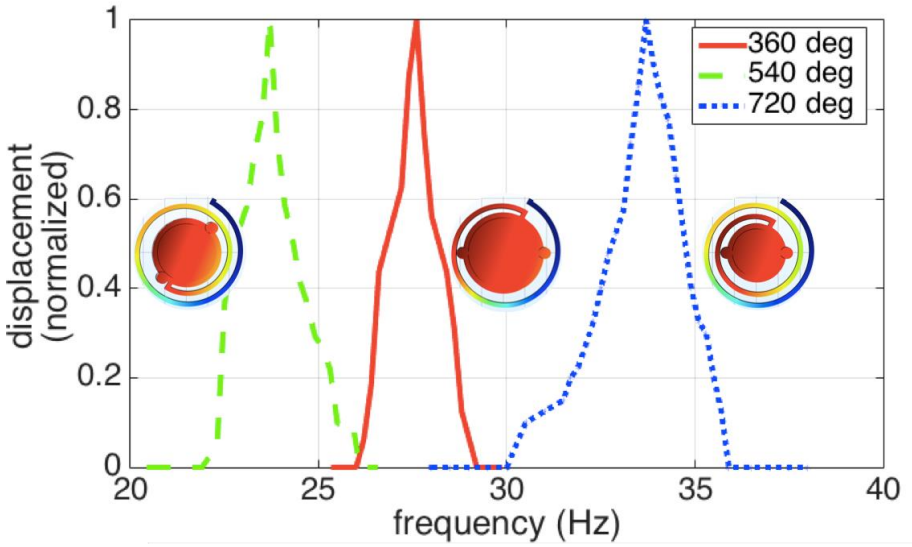

Figure 5.1 : Measured mechanical frequency response of 1, 1.5, and 2 turn spiral actuators. Insets illustrate fundamental mode shapes for each device.

Using the same setup in figure 4.1.1 the actuator displacement was observed with the side camera as a function of applied power to the coil (figure 5.2). We note that a 100-μm actuator displacement was observed for an applied power of ~1 mW, which corresponds to 1.6 mm of focal shift at the target when the longitudinal magnification (M_L = 16) is considered. The capability of adjusting the focus for the 1.6 mm range ensures addressing all of the Mucosa, Muscularis Mucosae, Submucosa, Circular, and longitudinal muscle layers of the small intestine.

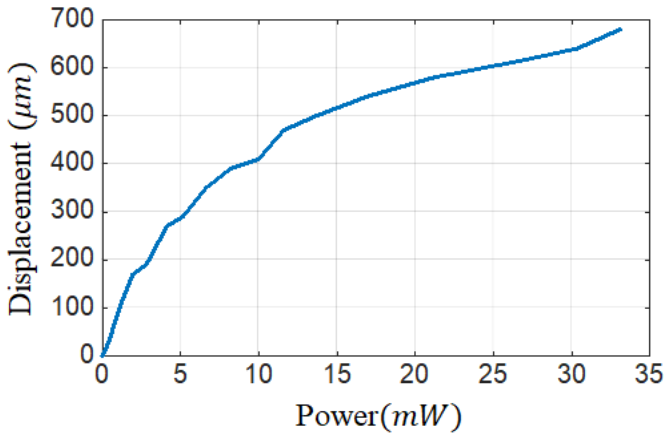

Figure 5.2 : Testing the tuning capability of the 540° actuator. The displacement of the actuator vs. power required for actuation

The CMOS camera (CAM) in figure 4.2 was placed at the target plane, at a 25 mm distance from the lens, to observe the focal spot as a function of time. The actuator drive voltage was then readjusted to obtain a focal shift of ±2.5 mm (5 mW power was supplied to the coil). The camera was initially placed at 25 mm (middle frame in Figure 5.3), where the laser was focused when the actuator is at its rest position (t = 0). The focus shifts to 22.5 mm and 27.5 mm, respectively, at a quarter-period before and after the rest position. Thus, the laser spots appear larger at the CMOS camera. Figure 5.4 illustrates the spot profile, which shows a 12 μm FWHM (full-width half-maximum) diameter. The observed spot profile is near 4x larger than the analytically calculated spot diameter. This is attributed to a combination of i) using an in-capsule laser diode having a large M^2 value and an elliptic beam profile and to ii) the utilized lens having a 22% smaller clear aperture as opposed to its outer diameter, and iii) the focused spot being further away from the lens (at 25 mm) rather than that planned for use in small intestine (focal spot at 17 mm away from the lens). In the upcoming experiments that required signal acquisition from the target, the laser diode was coupled into a single-mode fiber for both laser delivery into the capsule and data acquisition from the target.

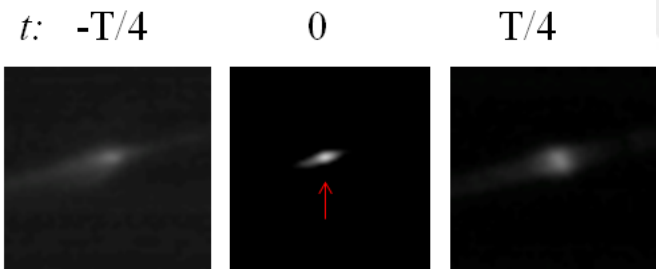

Figure 5.3 : focal spot as observed at different times (at t=0 the spot is in focus at f) and for the upper and lower raw frames, the camera is adjusted $\pm 2{,}5\ mm$ to capture the focus.

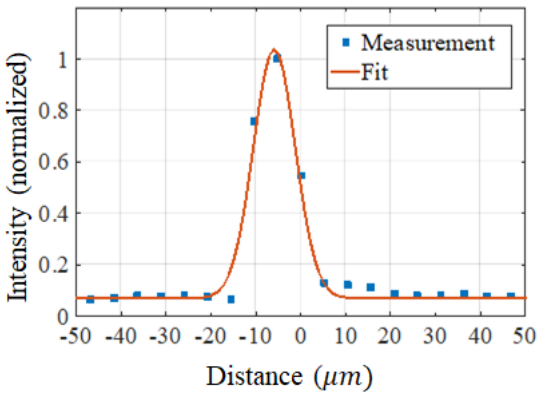

Figure 5.4 : spot profile of the diode laser at focus point.

Finally, we focused on the data acquisition from the two mirrors placed across each other (180 degrees apart) shown in figure 4.3. Initially, the mirrors were placed equidistant (25 mm away) from the capsule. As expected, two spikes were observed for each motor period (T), at t= T/4 and 3T/4, respectively, as illustrated in figure 5.5.a. Next, the actuator was turned on (driven at 5T, likewise shown in figure 3.1 while the mirror positions were retained. Both spikes arriving from each mirror were modulated to be in-phase, such that they appear and disappear in the same motor periods (figure 5.5. b). Finally, we move one of the mirrors by 5 mm such that they are no more equidistant. For the updated mirror positions, spikes coming from each mirror are modulated to be out-of-phase. Consequently, the signal from only one of the mirrors is observed at each motor period (either from M_1 or M_2).

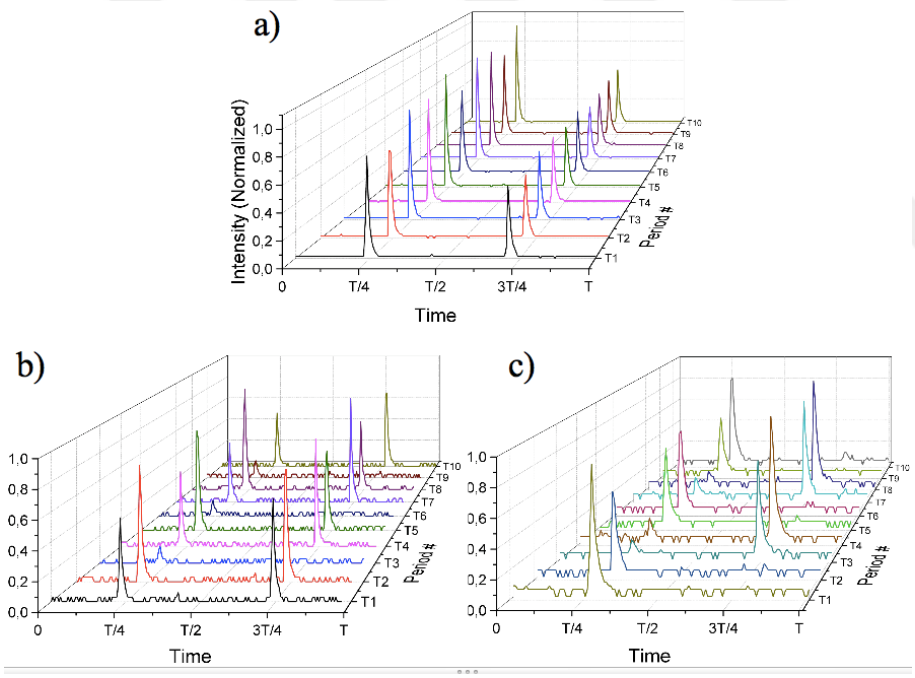

Figure 5.5 : Data acquisition from the target for ten motor periods, comprising two mirrors placed across each other a) Motor ON, actuator OFF, mirrors are equidistant b) Motor ON, actuator ON, mirrors are equidistant c) Motor ON, actuator ON, mirrors are at different distances to the lens.

6. OTHER CAPSULE SUBSYSTEMS

Throughout the manuscript, we have focused on the optical and mechanical aspects of the capsule. In this section, we give a summary of the interconnections between optical, micromechanical, electronic, and antenna subsystems. A system-level block diagram of the wireless laser scanning capsule endoscope is shown in Figure 6.1. Accordingly, the integrated electronics subsystem is responsible for i) driving the laser [21] and the coil; ii) converting the photodiode current output to voltage via a transimpedance amplifier (TIA), iii) quantizing it with an analog-to-digital converter and subsequently modulating it at an ISM frequency (433 MHz) by employing an injection-locked ring oscillator and its collateral circuits [22], iii) filtering signals outside the required bandwidth through impedance matching between blocks, and iv) power amplification of the signal so that it can be radiated with high efficiency from the transmitter antenna. The receiving on-body unit will be equipped with a receiver antenna and circuit modules, including a low-noise amplifier (LNA), mixer, filters, and analog/digital signal processing blocks. Furthermore, a single feed- dual meandered loop transmitter antenna was designed and implemented at 433 MHz to establish circular polarization [23]. We were able to show a wide circular polarization bandwidth (50%) and also beamwidth (showcasing circular polarization, i.e., an axial ratio of < 6dB, over a 246° azimuthal angle), offering data transmission throughout a wide variety of capsule orientations and tissue compositions.

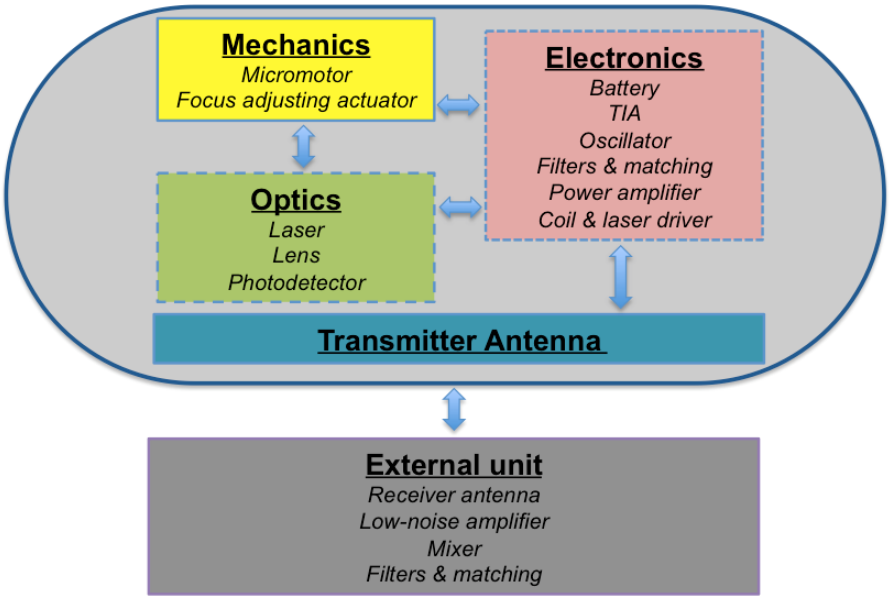

Figure 6.1 : Block diagram of the wireless laser scanning capsule endoscope.

7. CONCLUSION

In this thesis, we have presented laser-scanning wireless capsule endoscope architecture. We have thoroughly discussed the design, manufacturing, and testing results of a 3D-printed focus adjustment actuator. The developed actuator was embedded within a capsule unit, where different target acquisition scenarios (motor ON actuator OFF, motor ON actuator ON single layer readout, motor ON actuator ON multiple-layer readout) were implemented. Finally, we discuss ongoing work on integrated electronic and antenna subsystems towards achieving the laser scanning capsule prototype. With further development, the proposed device can provide multi-layered sub-cellular resolution images of difficult-to-access sites (i.e., the small intestine) within the gastrointestinal tract.

REFERENCES

[1] **P.B. Cotton, C.B. Williams, R.H. Hawes, B.P. Saunders**. (2009). Practical Gastrointestinal Endoscopy: The Fundamentals: Sixth Edition, doi:10.1002/9781444300819.

[2] **Y. J. Yang.** (2020). The Future of Capsule Endoscopy: The Role of Artificial Intelligence and Other Technical Advancements. *Clinical endoscopy*, *53*(4), 387–394. https://doi.org/10.5946/ce.2020.133

[3] **C. Ell, et al.** (2002). The first prospective controlled trial comparing wireless capsule endoscopy with push enteroscopy in chronic gastrointestinal bleeding, Endoscopy. 34. 685–689. doi:10.1055/s-2002-33446.

[4] **M.J. Gora, et al.** (2013). Tethered capsule endomicroscopy enables less invasive imaging of gastrointestinal tract microstructure, Nat. Med. 19. 238–240. doi:10.1038/nm.3052.

[5] **G.J. Ughi, et al.** (2016). Automated segmentation and characterization of esophageal wall in vivo by tethered capsule optical coherence tomography endomicroscopy, Biomed. Opt. Express. 7. 409. doi:10.1364/boe.7.000409.

[6] **J. Krause, P. A. Bhounsule.** (2018). 3D Printed Linear Pneumatic Actuator for Position, Force and Impedance Control. *Actuators*, *7*, 24. https://doi.org/10.3390/act7020024

[7] **Ye Wang et al.,** (2018). "3D printed fiber optic faceplates by custom controlled fused deposition modeling," Opt. Express 26.

[8] **J. Savas, et al.** (2018). “Towards fully 3D-printedminiaturized confocal imager”, Optical Engineering.

[9] **R. Bazaz, S., Rouhi, O., Raoufi, M.A. *et al.*** 3D Printing of Inertial Microfluidic Devices. *Sci Rep* 10, 5929 (2020). https://doi.org/10.1038/s41598-020-62569-9

[10] **N. Shahrubudin, et al.** (2019). An Overview on 3D Printing Technology: Technological, Materials, and Applications, Procedia Manufacturing, Volume 35, ISSN 2351-9789, https://doi.org/10.1016/j.promfg.2019.06.089.

[11] **X. Xu, et al** (2020). Stereolithography (SLA) 3D printing of an antihypertensive polyprintlet: Case study of an unexpected photopolymer-drug reaction, Additive Manufacturing, Volume 33.

[12] **A. Goyanes, et al.** (2016). 3D scanning and 3D printing as innovative technologies for fabricating personalized topical drug delivery systems, Journal of Controlled Release, Volume 234.

[13] **G. Kollamaram, et al.** (2018). Low temperature fused deposition modeling (FDM) 3D printing of thermolabile drugs, International Journal of Pharmaceutics, Volume 545, Issues 1–2.

[14] **P. DUDEK.** (2013). FDM 3D PRINTING TECHNOLOGY IN MANUFACTURING COMPOSITE ELEMENTS. Archives of Metallurgy and Materials. Vol 58. DOI: 10.2478/amm-2013-0186

[15] **L. Xie, P. Ko, R. Du.** (2014). The mechanics of spiral springs and its application in timekeeping, J. Appl. Mech. Trans. ASME. 81. doi:10.1115/1.4024669.

[16] **B.E.A. Saleh, M.C. Teich,** Fundamentals of Photonics, 2nd Edition, Wiley. (2007) 1200.

[17] **H.F. Helander, L. Fändriks.** (2014). Surface area of the digestive tract-revisited, Scand.J.Gastroenterol.49.681–689. doi:10.3109/00365521.2014.898326.

[18] **E. Hecht,** (2001). Optics 4th edition, Opt. 4th Ed. by Eugene Hecht Read. MA Addison-Wesley Publ. Co. 2001. 1. 122. doi:10.1119/1.3274347.

[19] **H.J. Wei, D. Xing, G.Y. Wu, Y. Jin, H.M. Gu,** (2003). Optical properties of human normal small intestine tissue determined by Kubelka-Munk method in vitro, World J. Gastroenterol. 9 .2068–2072. doi:10.3748/wjg.v9.i9.2068.

[20] **J. WorsØe, et al.** (2011). Gastric transit and small intestinal transit time and motility assessed by a magnet tracking system, BMC Gastroenterol. 11. doi:10.1186/1471-230X-11-145.

[21] **T.Ö. D, O. Ferhanoğlu, M.B. Yelten,** (2021). Design of a Constant Current Laser Driver for Biomedical Applications, IEEE Lat. Am. Symp. Circuits Syst.

[22] **M. Berk, B.B. İnam, M.B. Yelten.** (2021). An ISM-Band Multi-Phase Injection-Locked Ring Oscillator, in IEEE Lat. Am. Symp. Circuits Syst., Arequipa.

[23] **E. Güreş, M.B. Yelten, Ö. Özdemir, O. Ferhanoğlu.** (2021). A meandered dual loop antenna for wireless capsule endoscopy, AEU - Int. J. Electron. Commun. doi:10.1016/j.aeue.2021.153792.

CURRICULUM VITAE

Name Surname : İsraa Salaheldin

EDUCATION :

- **B.Sc.:** 2018, Istanbul Technical University, Faculty of Science and Letters, Department of Physics Engineering

PUBLICATIONS ON THE THESIS:

- **İ. Salaheldin, et al.** "Wireless Laser Scanning Capsule Endoscopy: A Preliminary Study on Device Architecture, Lens Actuator, and Future Prospects" submitted to Sensors and Actuators A, in May 2021.

- **İ. Salaheldin, et al. "**A 3D-Printed Archimedean Actuator for Focus adjustment in Endoscopes". Presented as a Poster in European Conferences on Biomedical Optics. SPIE/OSA. June 2021